KSME International Journal, Vol. 13, No. 10, pp. 727~737, 1999

Control of Linear Motor Machine Tool Feed Drives for End Milling: Robust MIMO Approach

Chintae Choi*, Keum-Shik Hong*, Joongwan Kim** and Jong Shik Kim*****

(*Received January 25, 1999*)

Linear motors become promising for use as high speed, high accuracy machine tool feed drives. The cutting force in the machining process are directly reflected to the linear motor due to no gearing mechanism. To achieve highly accurate machining, the controller for the linear motor system should be designed to compensate for the cutting force.

In this work, a MIMO H_∞ controller for the linear motor machine tool feed drives has been designed to reduce tracking errors induced by cutting forces for end milling. The controller is designed using normalized coprime factorization method for the dynamic model of the linear motor system. The model includes constant in-line and cross coupling force gain, since the feedback cutting force can be considered as the product of the constant gain and the moving velocity of each axis. Analysis of the structured singular value shows that the designed controller has good robust performance despite wide variations of the cutting force and physical parameters. It is directly implemented on a linear motor X-Y table which is mounted on a milling machine to have cutting experiments via a DSP board. Experimental results verified effectiveness of the proposed scheme to suppress the effects of the cutting force in the high feed rate.

Key Words: Linear Motor, Machine Tool, End Milling, Control

1. Introduction

High speed machining is getting more desirable to improve productivity. Directly driven feed drives can eliminate detremental effects of backlash and structural flexibilities due to gear reduction mechanism. It seems that linear motors can be used as good machine tool feed drives due to their high acceleration and direct driving capabilities. The feed drive and the cutting process in the end milling are coupled, because the linear motor system has no gearing mechanism. While the elimination of gearing gives benefit of high speed tracking, the cutting forces are directly applied to the motors due to the direct coupling and have severe effect on the tracking accuracy. The Coulomb friction are also more prominent for the linear motors. The higher the stiffness becomes, the better the linear motor can bear the external disturbances. The stiffness is determined by the feedback loop gain of the individual servomechanism. For a gear-drive system, the loop gain increases with the gear ratio since the motor output torque is amplified by the gear reducer. The linear motor system, however, cannot take this advantage of the reducer. Consequently, the linear motor needs a higher controller gain to compensate for the deficiency of the loop gain.

Another problem of the linear motor system is that it has almost zero damping, which may cause difficult problem in the control system design. Mechanical damping is produced only at the linear bearings supporting the moving table connected to the linear motor. The mechanical time constant of the linear motor system is even larger than that of the gear reduction mechanism,

* Mechanical & Electrical Engineering Team, RIST
** Department of Mechanical Engineering, Dong-A University
*** School of Mechanical Engineering, Pusan National University

because it is the ratio of the inertial load to the damping coefficient. Therefore, damping of the feedback system has to be increased by the controller.

Alter and Tsao(1994 and 1996) investigated the use of linear motors as feed drives for the turning process. They showed that the system stability is primarily dependent on the interaction of the cutting process and the feed drive servo loop in a direct drive. The cutting force in the end milling process is primarily periodic with DC component due to the rotating flutes. The frequency of the periodic force is mostly outside of the closed loop system bandwidth. For example, the tooth passing frequency of spindle rotating at 3000 rpm with a 2 flute cutter is 100 Hz, but closed loop system bandwidth for the machine tool is under 30 Hz. Accounting for the average force component would be sufficient to reduce tracking errors due to cutting. The average forces in the in-line and cross directions was obtained by integrating the instantaneous forces over the duration of the cutting passes (Golub, 1992).

Linear motors in the X-Y table are highly coupled due to lack of gearing mechanism and characteristics of the cutting process which generates forces in the direction of a feed drive without movement command in the milling process. Therefore, the tracking control of linear motors in the end milling process results a multi-input multi-output(MIMO) system. Cutting forces greatly varies according to cutting conditions. They are highly dependent on feed rate, cutting depth and material of the workpiece. McNab (1997) addressed the control of linear motors machine tool feed drives for the end milling process, and showed that 2 axes end milling process is a MIMO system rather than two SISO systems with inclusion of in-line force and cross force feedback. The in-line and cross coupling force is expressed as the product of the constant in-line and cross coupling gain and the moving velocity of each axis, respectively.

A MIMO H_∞ controller for X-Y table system using linear motors as machine tool feed drives in the end milling process is suggested to improve the tracking accuracy in this research. The dynamic model of the X-Y table system is considered as a 2 input 2 output system coupled by the constant force gain for the cross force feedback. The controller with high gain is designed to increase stiffness of the system and reduce tracking error induced by the cutting forces. The feedback force gains are considered to have parametric uncertainties and therefore robust controller is designed using loop shaping method with the normalized coprime factorization. Robustness of stability and performance for parametric changes of the force gains and the physical parameters including unmodeled power amplifier dynamics is examined using structured singular values. The designed MIMO controller is also compared with two SISO controllers for x and y axes, which do not consider the coupled force terms between axes. The SISO controllers are designed by the conventional loop shaping method to have the similar loop shape and robust stability to the MIMO one. Simulation and experimental results verify that the closed loop system maintains its robustness in spite of wide changes of force gains and the MIMO controller has better performance to suppress tracking errors than the SISO controllers.

2. Modeling of the Linear Motor System

Neglecting the dynamics of the electrical parts in the linear motor X-Y table, its velocity model can be represented as the 1st-order differential equation for each axis

$$\dot{v}_i+\frac{b_i}{m_i}v_i+\frac{F_{Coul,i}}{m_i}sign(v_i)=\frac{k_i}{m_i}u_i, \quad (1)$$

where v is velocity, m is mass, b is viscous damping, k is input gain, is Coulomb friction and $i=x$, y, respectively.

There have been a lot of researches on the cutting force model for end-milling operation (Tlusty and MacNeil, 1975; Devor et al, 1980), but they are complicated for control purpose. The cutting force is basically composed of 2 frequency components, the DC component and the other at the tooth passing frequency. We assume that for

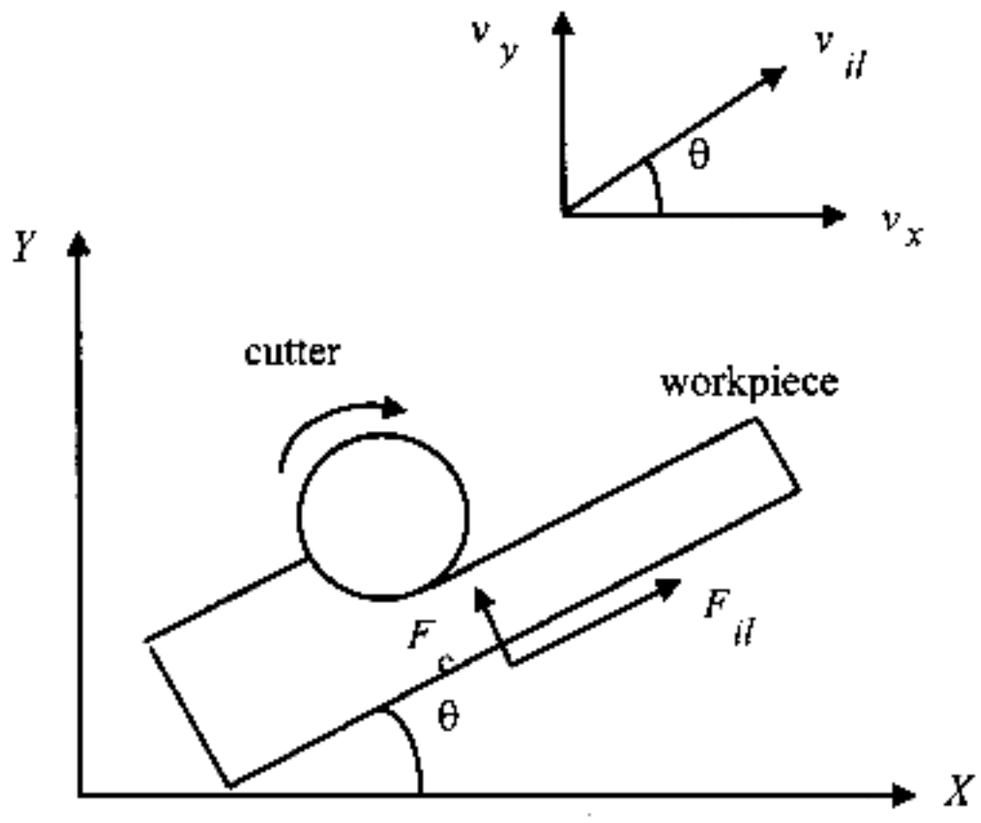

Fig. 1 Cutting forces applied to a workpiece.

the average force component would be sufficient for reducing the tracking errors during cutting, since the cyclic component amplitude of the tool force does not exceed 20% of its average value (Golub, 1992). The average forces in the in-line and cross directions were obtained by integrating the instantaneous forces over the duration of the cutting passes. The average forces are expressed, as shown in Fig. 1, to be

$$F_{il}=k_{il}v_{il}, \tag{2}$$

$$F_c=k_cv_{il} \tag{3}$$

where F_{il} and F_c are the forces in the in-line and cross directions, and k_{il} and k_c are in-line cutting force gain and cross coupling force gain, respectively.

Obtaining the cutting forces for each axis,

$$\begin{aligned} F_x&=F_{il}\cos\theta-F_c\sin\theta\\ &=k_{il}v_{il}\cos\theta-k_cv_{il}\sin\theta\\ &=k_{il}v_x-k_cv_y \end{aligned} \tag{4}$$

$$\begin{aligned} F_y&=F_{il}\sin\theta-F_c\cos\theta\\ &=k_{il}v_y+k_cv_x \end{aligned} \tag{5}$$

Each axis of the linear motor X-Y table including the cutting force in the milling process is modeled as

$$\begin{aligned} &\dot{v}_x+\frac{b_x}{m_x}v_x+\frac{F_{cout,x}}{m_x}sign(v_x)\\ &=\frac{k_x}{m_x}u_x+k_{il}v_x-k_cv_y, \end{aligned} \tag{6}$$

$$\begin{aligned} &\dot{v}_y+\frac{b_y}{m_y}v_y+\frac{F_{cout,y}}{m_y}sign(v_y)\\ &=\frac{k_y}{m_y}u_y-k_{il}v_y+k_cv_x, \end{aligned} \tag{7}$$

The dynamic model for the 2 axes has 2 input 2 output structure coupled by the cross coupling forces.

3. H_∞ Loop Shaping Controller Design

This approach makes use of an uncertainty description based on additive perturbation to a normalized coprime factorization of the plant (Glover and McFarlane, 1989). It is particularly attractive in that the optimal ∞-norm γ can be found without recourse to the γ-iteration which is normally required to solve H_∞ problems. Given a minimal realization $[A, B, C, 0]$ of a controllable and observable plant including a loop compensator W_s, the central controller is given by

$$K=\left[\begin{array}{c|c} A-ZC^*C+\gamma^2BB^*X(I+XZ-\gamma^2I)^{*-1} & \\ \hline \gamma^2B^*X(I+XZ-\gamma^2I)^{*-1} & \end{array}\right.\left.\begin{array}{c} \\ \hline \dfrac{ZC^*}{0} \end{array}\right] \tag{8}$$

where X and Z are the solutions of the Control Algebraic Riccati Equation and Filtering Algebraic Riccati Equation, respectively. Choosing ∞-norm γ to be slightly suboptimal can give a great improvement in H_2 performance, and also avoids introducing a fast pole into the controller. The controller design procedure by this method gives a good idea of what performance is achievable with a particular plant. Even though μ synthesis can ensure robust performance with $\mu\leq 1$, the order of the resulting controller is considerably high and γ-iteration should be done to find γ to satisfy the existence of the solution. The H_∞ Loop Shaping method gives a controller near to $\mu=1$ without γ-iteration. Robust stability and robust performance for the controller are examined by μ analysis in the later section, even though the controller is designed by the H_∞ loop shaping method.

Using a loop compensator the magnitude of the nominal system G is shaped to give a desired target loop which determines the open-loop shape of the closed-loop system. Noting that performance is usually required at low frequencies and robustness at high frequencies, the target open loop of the closed-loop system should

have high amplitude at low frequencies and low amplitude at the high frequencies. The selection of the target loop is based on the familiar SISO loop- shaping guidelines. Shaping a crossover roll-off rate close to −20db/dec is consistent with Bode's observation that roll-off rate determines phase, and that a rate of -20db/dec corresponds to 90 degrees of the phase.

Obtaining the error signal for the external disturbance force reflected on the entry side of the linear motor system,

$$e=(I+GK)^{-1}Gf \tag{8}$$

where e is an error, K is a controller and f is a disturbance, respectively. The norm of the error is

$$\| e \|=\|(I+GK)^{-1}Gf \| \leq \|(I+GK)^{-1}G\| \|f\| \tag{9}$$

If Euclidean norm is used for e and f, $\|(I+GK)^{-1}G \|=\bar{\sigma}((I+GK)^{-1}G)$ where $\bar{\sigma}$ denotes the maximum singular value. At low frequencies such that $\underline{\sigma}(GK)\gg 1$, the approximations $\bar{\sigma}((I+GK)^{-1}G)\cong 1/\underline{\sigma}(K)$ can be made and $\| e \|\leq \| 1/\underline{\sigma}(K)\|\|f\|$. A controller with high gain in low frequencies is desirable to reduce tracking errors. A loop compensator should be selected so that the final feedback controller would have high gain. But a high gain in the controller may result in wide bandwidth of the system, which may allow that the frequency of the cyclic component of the cutting force by the rotating spindle exists inside of the system bandwidth. Therefore, there should be a compromise between the gain selection and the system bandwidth so that the feedback system does not have effects by the cyclic forces of the rotating tool.

$W_s=diag\{990(s+110)/(s+1500),\ 660(s+110)/(s+1500)\}I_{2\times 2}$ in this design gives the target loop a high gain in the low frequencies region and -20db/dec. roll-off rate near the cut -off frequency as shown in Fig. 2. In the later cutting experiments, the spindle speed of a 2 flutes cutter will be 5000 and 10000 rpm, respectively, which correspond to about 167 and 333 Hz of the tooth passing frequency, respectively. Therefore, the designed controller can sufficiently suppress the cyclic cutting forces. The proportional gains

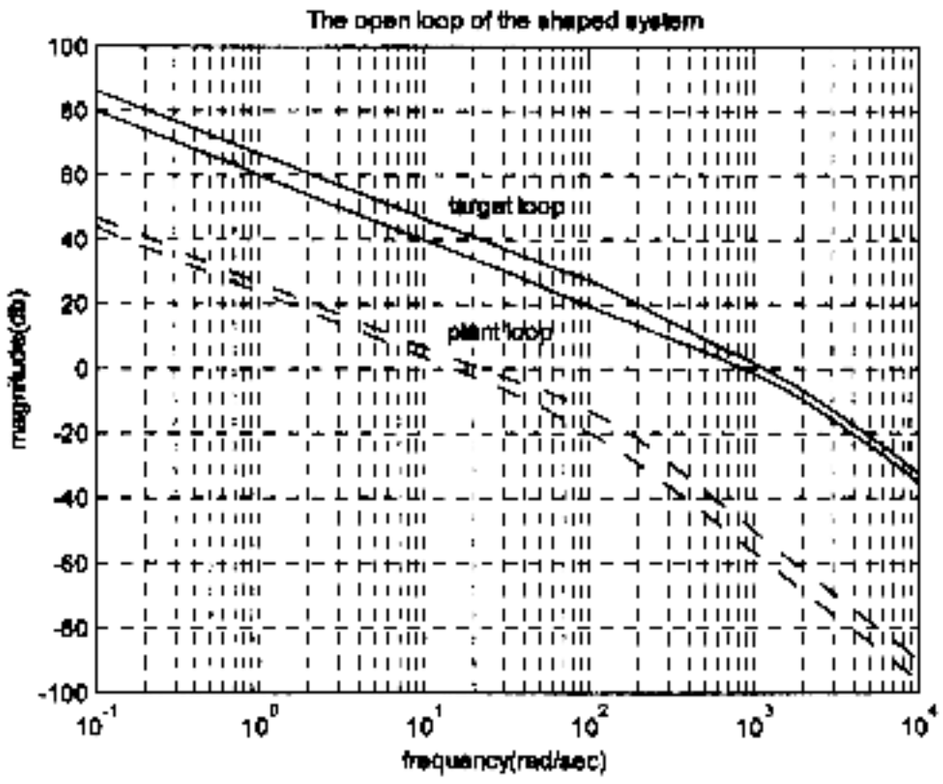

Fig. 2 The open loop and target loop of the system.

for both axes are selected so that they have the similar response time. Introduction of the zero into the loop compensator may increase damping of the system to compensate for the deficiency of the mechanical damping in the linear motor axis. The open loop gain of the linear motor system in the singular value plot went up by the loop compensator with high gain, compared with the plant open loop, and the target loop has considerably high amplitude in the low frequencies.

The order of the designed MIMO controller is 8, but is reduced to 4 by Schur balanced truncation method to reduce the execution time in the DSP board.

4. Analysis of Robustness

Robust stability is highly desirable in this system, because some parameters of its dynamic model vary widely. Actual values of physical parameters m, b, k_{il} and k_c are not known exactly, but are believed to be in known intervals. Especially, the cutting force gains are highly dependent on axial depth, radial depth, cutting angle, etc. and have greater variations than other parameters. Therefore, it is not needed to obtain and compensate for their exact values. Robust control approach which allows their variations in predetermined intervals will be more reasonable for real implementation.

Expressing actual values of all the parameters with multiplicative uncertainties,

$$m_{a,x}=m_x(1+\alpha_{mx}\delta_{mx})$$

$$b_{a,x}=b_x(1+\alpha_{bx}\delta_{bx})$$
$$m_{a,y}=m_y(1+\alpha_{my}\delta_{my})$$
$$b_{a,y}=b_y(1+\alpha_{by}\delta_{by})$$
$$k_{il,a}=k_{il}(1+\alpha_1\delta_1)$$
$$k_{c,a}=k_c(1+\alpha_2\delta_2)$$

where perturbation $|\delta_i|\leq 1$. α_i is a constant that determines the limit of the known interval of actual parameter values. $\frac{1}{m_x}$ can be represented as LFT in δ_{mx} (Zhou, 1997).

$$\frac{1}{m_{a,x}}=\frac{1}{m_x(1+\alpha_{mx}\delta_{mx})}=\Gamma_l(M_{mx},\delta_{mx}) \quad (10)$$

with

$$M_{mx}=\begin{bmatrix}1/m_x & -\alpha_{mx}/m_x\\ 1 & -\alpha_{mx}\end{bmatrix}$$

where Γ_l is the linear fractional transformation.

The same will be done on the parameters of the y axis. The system block diagram including uncertainties is shown in Fig. 3. Define

$z=[z_{bx}\ z_{mx}\ z_{x1}\ z_{x2}\ z_{by}\ z_{my}\ z_{y1}\ z_{y2}]^T$, $y=[y_x\ y_y]^T$, $u=[u_x\ u_y]^T$, $x=[y_x\ v_x\ y_y\ v_y]^T$ and $w=[w_{bx}\ w_{mx}\ w_{x1}\ w_{x2}\ w_{by}\ w_{my}\ w_{y1}\ w_{y2}]^T$ where x, z, y and w are the system state, the regulated output, the measured output and the exogenous input, respectively. The state-space equations for the system with parametric uncertainties can be written as

$$\dot{x}=Ax(t)+B\begin{bmatrix}w(t)\\ u(t)\end{bmatrix}, \quad (11)$$

$$\begin{bmatrix}z(t)\\ y(t)\end{bmatrix}=Cx+D\begin{bmatrix}w(t)\\ u(t)\end{bmatrix}, \quad (12)$$

where

$$A=\begin{bmatrix}0 & 1 & 0 & 0\\ 0 & (k_{il}-b_x)/m_x & 0 & -k_c/m_x\\ 0 & 0 & 0 & 1\\ 0 & k_c/m_y & 0 & (k_{il}-b_y)/m_y\end{bmatrix},$$

$$B=\begin{bmatrix}0 & 0 & 0 & 0 & 0\\ -1/m_x & -a_{mx}/m_x & 1/m_x & -1/m_x & 0\\ 0 & 0 & 0 & 0 & 0\\ 0 & 0 & 0 & 0 & -1/m_y\\ 0 & 0 & 0 & 0 & 0\\ 0 & 0 & 0 & k_x/m_x & 0\\ 0 & 0 & 0 & 0 & 0\\ -a_{my}/m_y & 1/m_y & 1/m_y & 0 & k_y/m_y\end{bmatrix}$$

$$C=\begin{bmatrix}0 & \alpha_{bx}b_x & 0 & 0\\ 0 & k_{il}-b_x & 0 & -k_c\\ 0 & \alpha_1 k_{il} & 0 & 0\\ 0 & 0 & 0 & \alpha_2 k_c\\ 0 & 0 & 0 & \alpha_{by}b_y\\ 0 & k_c & 0 & k_{il}-b_y\\ 0 & 0 & 0 & \alpha_1 k_{il}\\ 0 & \alpha_2 k_c & 0 & 0\\ 1 & 0 & 1 & 0\\ 0 & 0 & 0 & 0\end{bmatrix},$$

$$D=\begin{bmatrix}0 & 0 & 1 & 0 & 0 & 0 & 0 & 0 & 0 & 0\\ -1 & -\alpha_{mx} & 0 & -1 & 0 & 0 & 0 & 0 & k_x & 0\\ 0 & 0 & 0 & 0 & 0 & 0 & 0 & 0 & 0 & 0\\ 0 & 0 & 0 & 0 & 0 & 0 & 0 & 0 & 0 & 0\\ 0 & 0 & 0 & 0 & 0 & 0 & 0 & 0 & 0 & 0\\ 0 & 0 & 0 & 0 & -1 & -\alpha_{my} & 1 & 1 & 0 & k_y\\ 0 & 0 & 0 & 0 & 0 & 0 & 0 & 0 & 0 & 0\\ 0 & 0 & 0 & 0 & 0 & 0 & 0 & 0 & 0 & 0\\ 1 & 0 & 0 & 0 & 0 & 0 & 0 & 0 & 0 & 0\\ 0 & 0 & 0 & 0 & 0 & 0 & 0 & 0 & 0 & 0\end{bmatrix}$$

Parametric uncertainties of the system gains k_x and k_y will be included in the unmodeled power amplifier dynamics, which is also considered as a multiplicative uncertainty.

The perturbed system can be described via the LFT so that all the uncertainty is represented as a nominal system with the unknown parameters as shown in Fig. 4.

Let G_t be the ten-input (w_{mx}, w_{bx}, w_{my}, w_{by}, w_{x1}, w_{x2}, w_{y1}, w_{y2}, u_x, u_y), ten-output (z_{mx}, z_{bx}, z_{my}, z_{by}, z_{x1}, z_{x2}, z_{y1}, z_{y2}, y_x, y_y), four-state nominal system shown in Fig. 4 and the unknown matrix $\Delta=diag\{\delta_{mx}, \delta_{bx}, \delta_{my}, \delta_{by}, \delta_1 I_{2\times 2}, \delta_2 I_{2\times 2}\}$, referred to as the perturbation, be structured.

The unmodeled power amplifier dynamics for each axis is assumed to be about 30% below 600 rad/sec frequency, rising to about 100 % at 2000 rad/sec, since it exists in the higher frequency region than the mechanical dynamics. Most of the modeling error below 600 rad/sec is assumed to be the error of the input gains k_x and k_y. A 2×2 transfer matrix, $W_s=\{(s+600)/(s+2000)\}I_{2\times 2}$ is chosen and δ_{dx} and δ_{by} are representing the related uncertainties for both axes. Performance robustness as well as stability robustness of the feedback system in the cutting should be

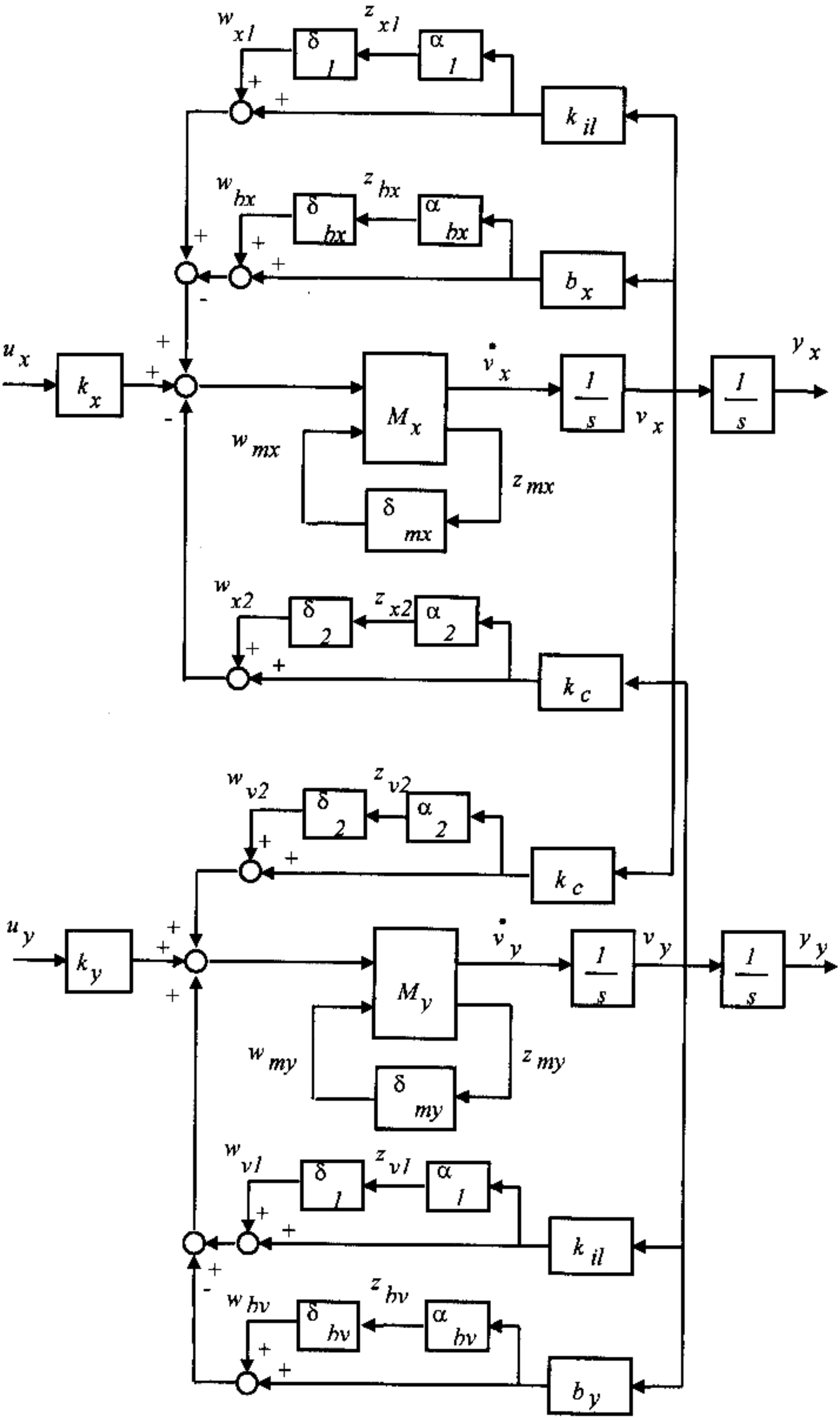

Fig. 3 The dynamic model of the X–Y table with uncertainties.

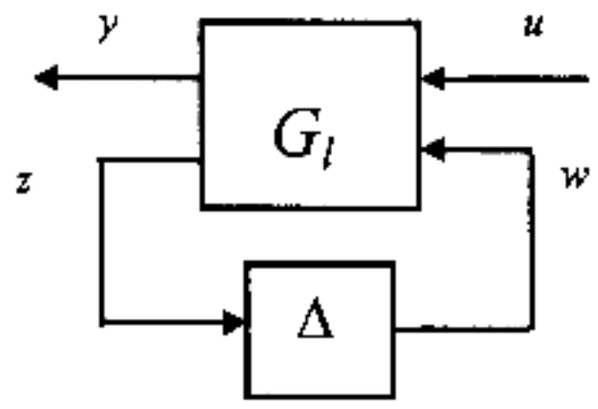

Fig. 4 LFT representation of the linear motor system with uncertainty.

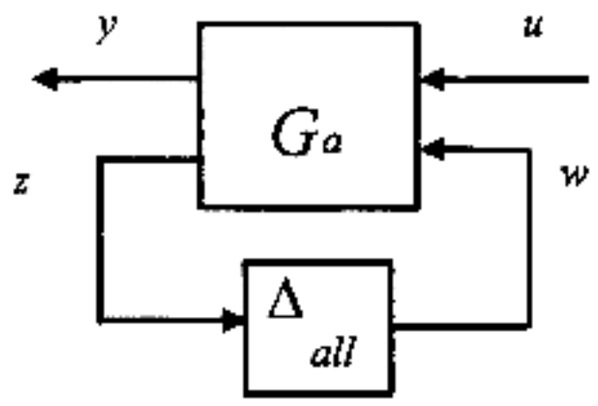

Fig. 5 Extended LFT representation for robust performance.

examined. Robust performance specification is assumed here that each linear motor axis should, under the parametric and unmodeled uncertainties and the excitation of uncertain exogenous signal, maintain the tracking error within 1/40 of the reference commands below 5 rad/sec. The tracking performance for the command is evaluated using the output sensitivity transfer function $(I+GK)^{-1}$. It is modeled by using a first-order 2×2 weighting matrix $W_p=\{2(s+100)/(s+5)\}I_{2\times 2}$ to satisfy $\|W_p(I+GK)^{-1}\|_\infty<1$. To evaluate robust performance, weights for tracking errors of the 2 axes with δ_{px} and δ_{py} are added into the generalized plant. The uncertainty matrix is defined as $\Delta_{all}=diag\{\Delta, \delta_{dx}, \delta_{dy}, \delta_{px}, \delta_{py}\}$ with the augmented generalized plant G_a as shown in Fig. 5(Balas et al, 1991). If the augmented generalized plant G_a has a structured singular value below 1 in all operating frequencies region, it is said to be robust in performance.

The physical parameters and their uncertainties used in this controller design is summarized in Table 1where k_{it} and k_c are chosen for up milling.

The closed-loop systems have small structured singular values and are sufficiently robust in the operating frequencies which are below about 80 rad/sec as shown in Fig. 6. It means that the closed-loop system is stable even though the

Table 1 Numerical values of the system parameters.

Parameters	Nominal value	Uncertainty (%)
k_{it}	−2500	110
k_c	2500	110
m_x	52.3	30
m_y	17	40
b_x	193.5	20
b_y	36	20

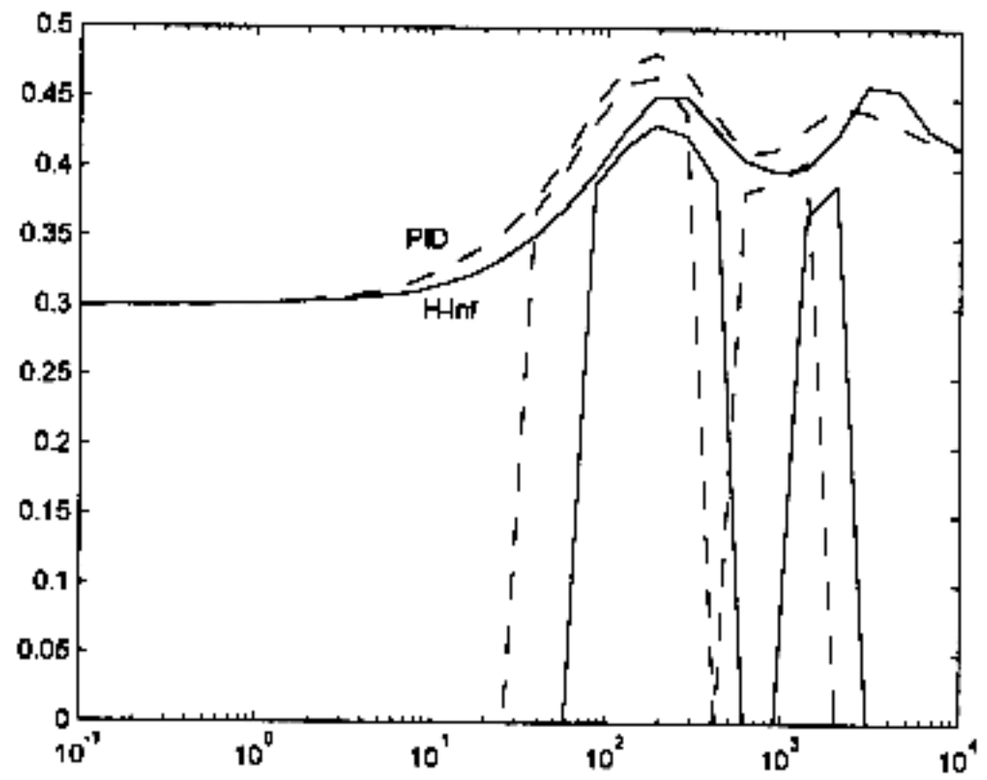

Fig. 6 Structured singular value for robust stability

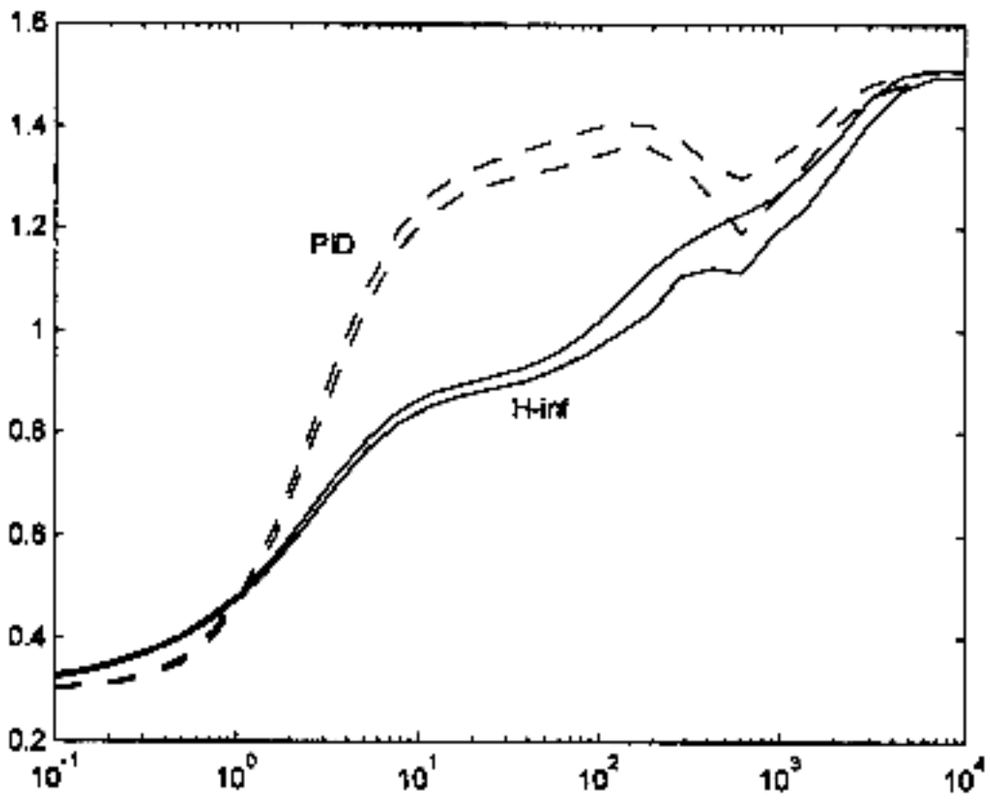

Fig. 7 Structured singular value for robust performance.

cutting force gains k_{it} and k_c vary from −5250 to 250 N/m/sec and from 5250 to −250 N(/m/sec), respectively, with variation of some physical parameters such as mass, damping coefficients etc. The MIMO controller is compared with a SISO PID controller to check its robustness and perfor-

mance. The PID controller considers the cutting forces as external forces. It is designed to have high gain for stiffness by using the conventional loop shaping. It shows similar structured singular values to the H_∞ one, which results in similar robust stability.

Another important ability that the controller should have is to suppress tracking errors induced by the moving command and external disturbances and keep this performances, regardless of the variations of the system model below the operating frequencies region. The structured singular value is a good measure to check robust performance of the controller. The H_∞ controller shows its performance robustness for the command and disturbances below 5 rad/sec and is superior to the PID as shown in Fig. 7.

5. Experimental Results

The linear motors used for the X-Y table are Anorad brushless linear servo motor LEB-S-8 for both axes and have the peak force of 982N and the continuous force of 349N, respectively. A 1 μm resolution linear encoder is mounted for the X axis which is the lower axis and a 2 μm resolution one for the Y axis. A Spectrum TMS320C30 DSP is used to execute the control algorithm written in C language. Control is implemented at a sampling rate of 2 KHz. The linear motor X-Y table was mounted and fixed on the bed of a Mori Seiki SV50 machining center as shown in Fig. 8. The vertical axis of the machining center with the rotating spindle moves up and down and its bed is fixed during the cutting. The linear motor X-Y table makes circles and lines during the cutting experiments.

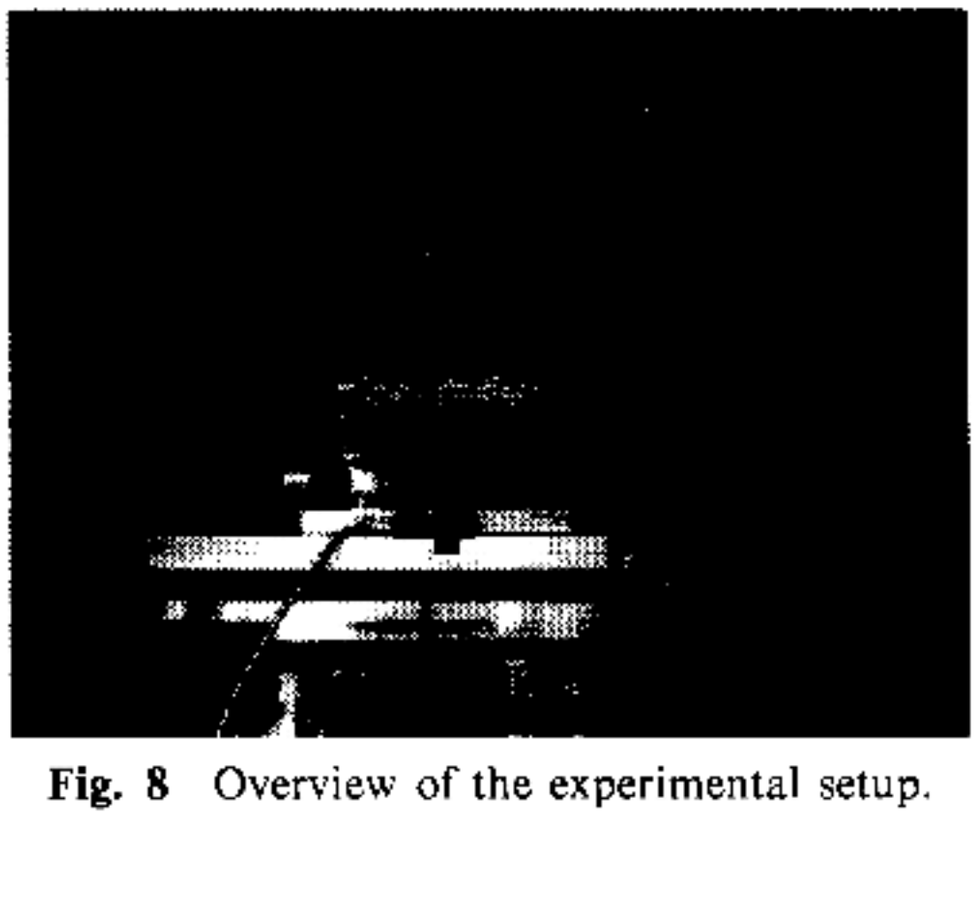

Fig. 8 Overview of the experimental setup.

A circular trajectory is examined in the air cutting. The radius of circle is 20 mm and the feed rate is 2400 mm/min. The MIMO controller

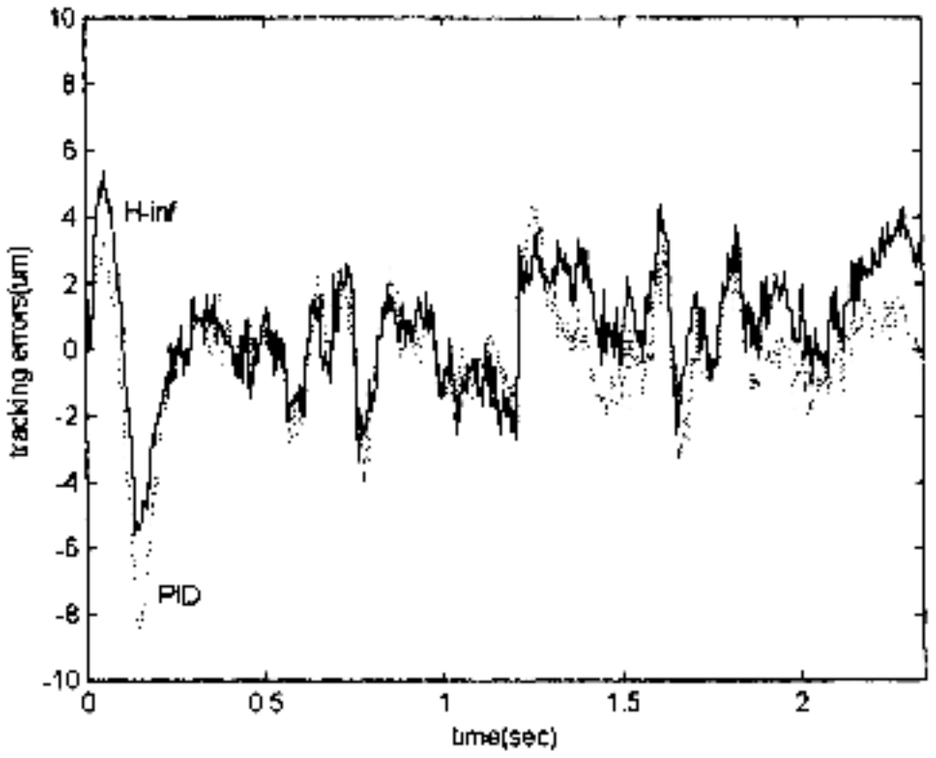

(a) Errors for the X-axis

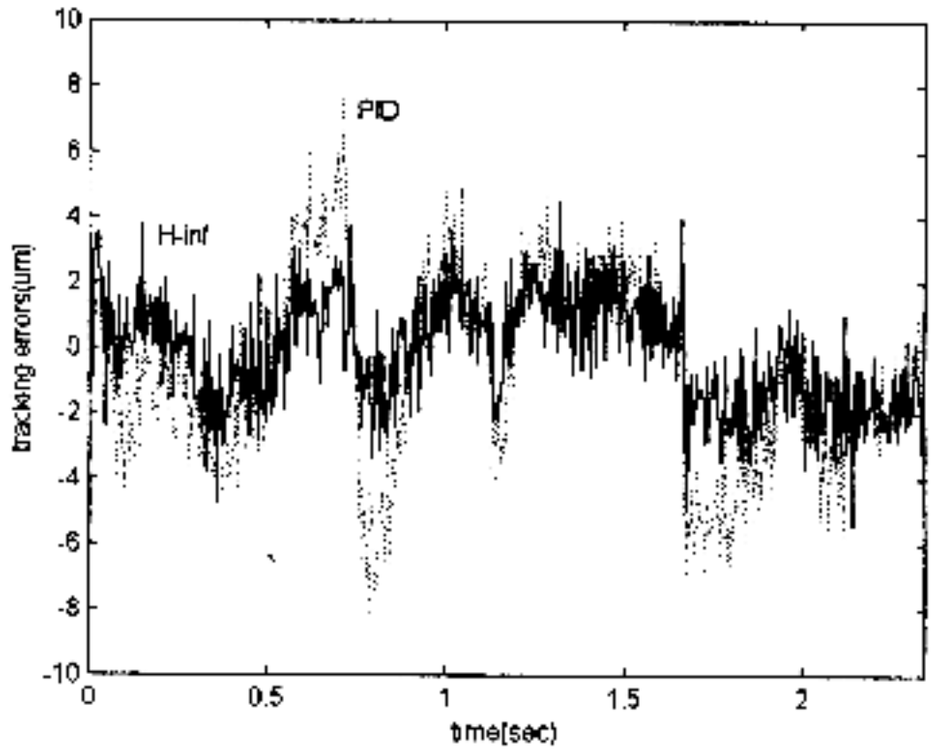

(b) Errors for the Y-axis

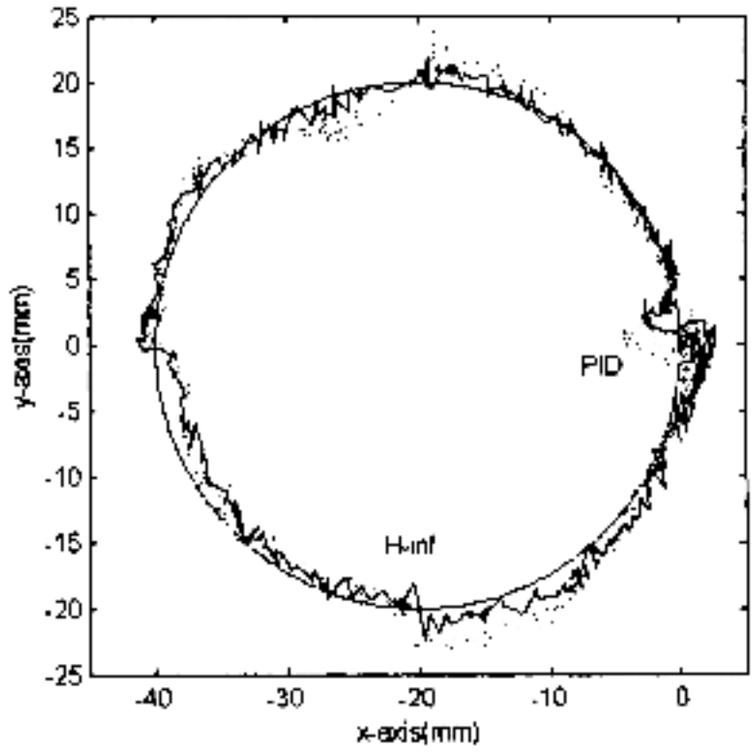

(c) Errors for the circle

Fig. 9 Comparison of the controllers in the air cutting.

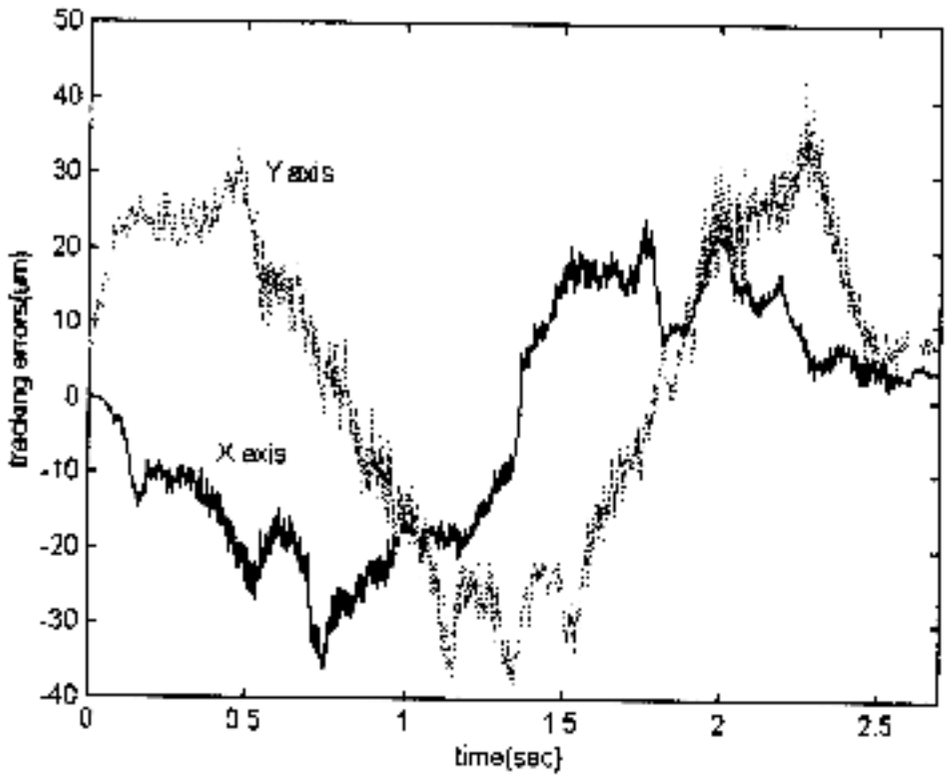

Fig. 10 Tracking errors for the MIMO controller.

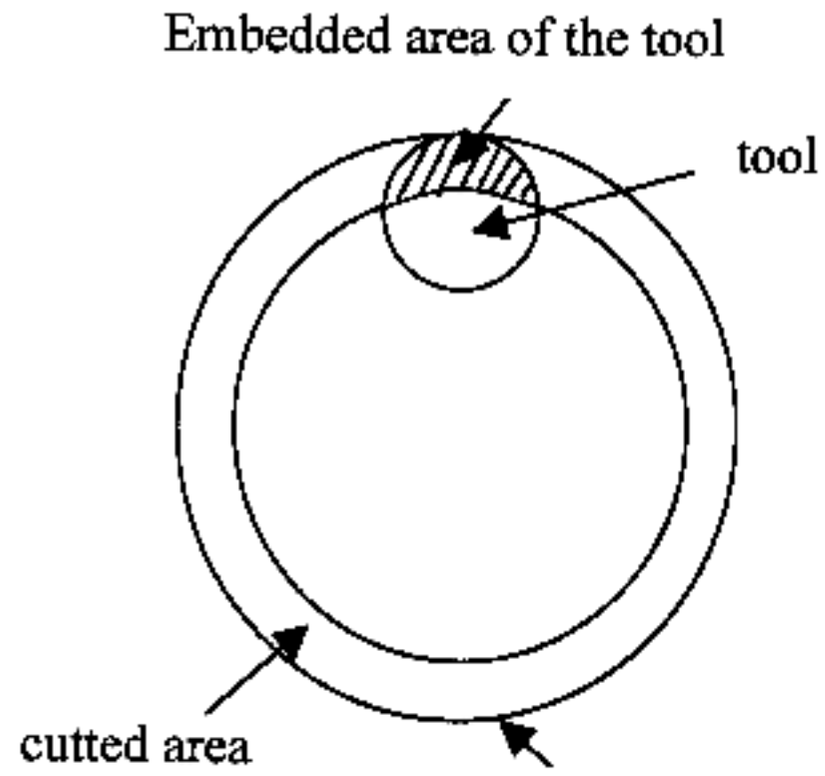

Fig. 11 Tool position in the circle cutting.

demonstrates a little better tracking performance for X and Y axes than the PID controller in the air cutting as shown in Fig. 9. The tracking controller consists of a feedback controller and a zero phase error tracking controller as a feedforward controller. The maximum tracking errors for both axes are less than 6 and 7 μm for the MIMO controller, respectively. The size of quadrant glitch at 90 degrees intervals around the circle is larger in the PID controller than in the MIMO controller. Even though the MIMO controller was designed by considering the cutting force gains k_{it} and k_c of -2500N/m/sec and 2500 N/m/sec, respectively, it shows good tracking performances in the air cutting which has no cutting forces.

A 2 flute end mill is used as a cutting tool in the cutting experiments and the workpiece is aluminum. A circle with the radius of 28 mm is

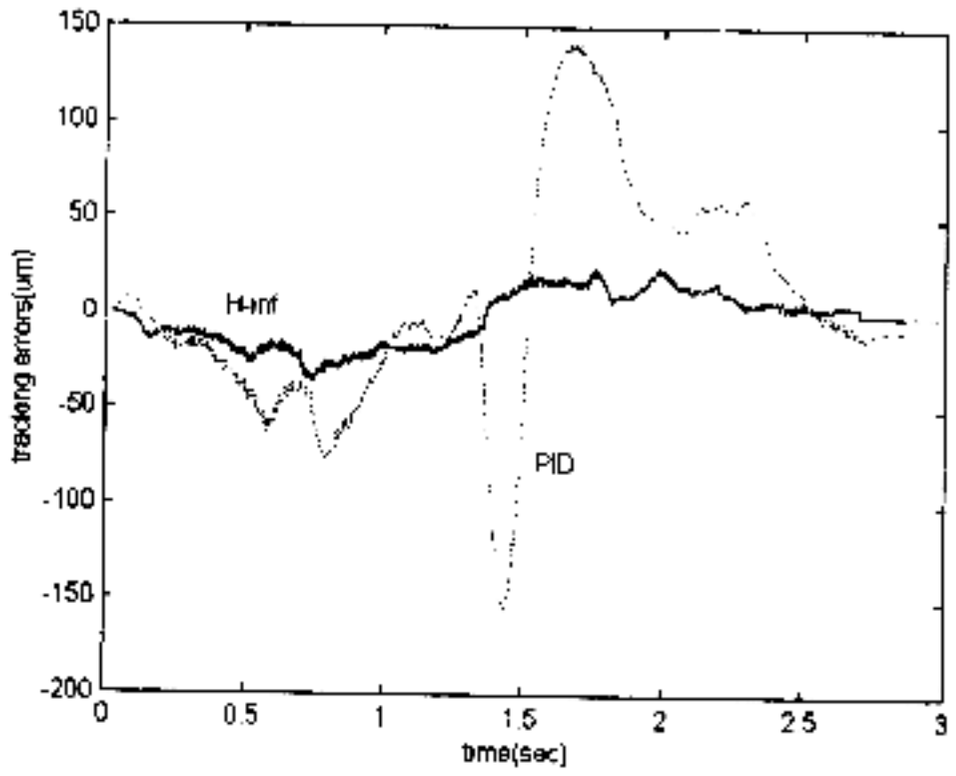

(a) Errors for the X axis

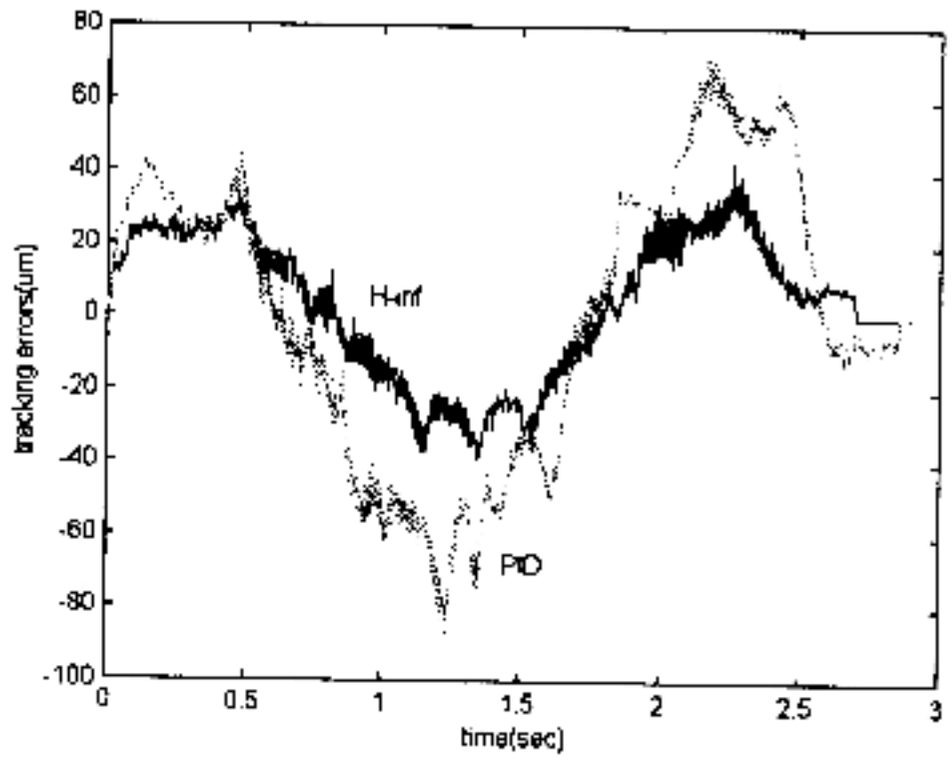

(b) Errors for the Y axis

(c) Errors for the circle

Fig. 12 Comparison of the contouring errors.

examined and the flute will cut the inner surface of the circle. The axial depth of cut, the radial depth of cut, the spindle speed and the feed rate of the table are 3mm, 3mm 10,000rpm and 4800 mm/min, respctively. This corresponds to a feed per tooth of 0.24 mm. Roughly estimating the cutting force gains for these cutting conditions (McNab,

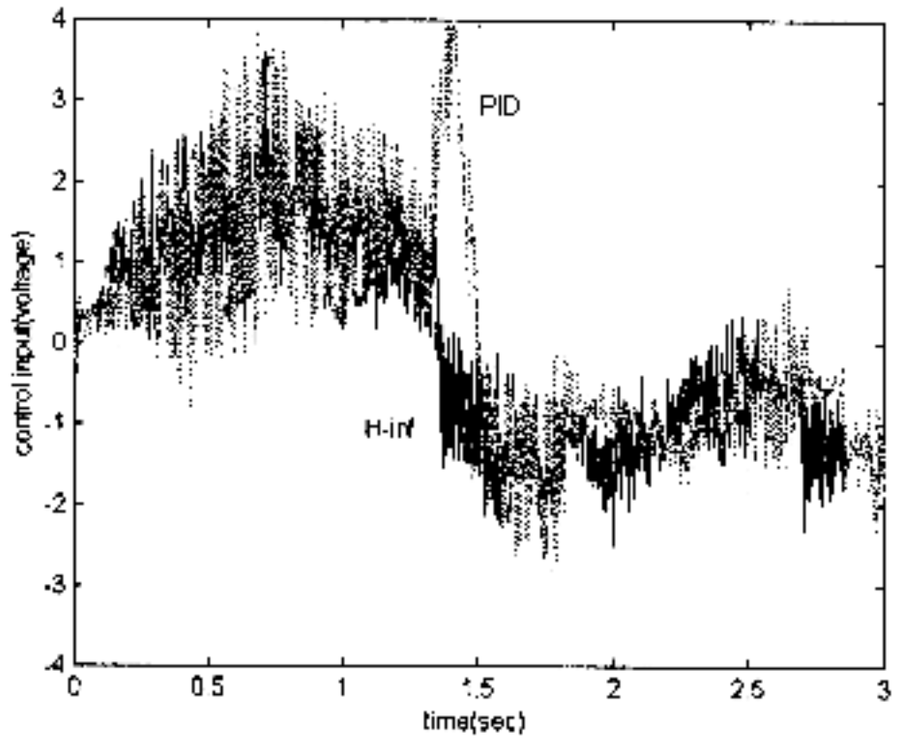

(a) Control input for the X axis

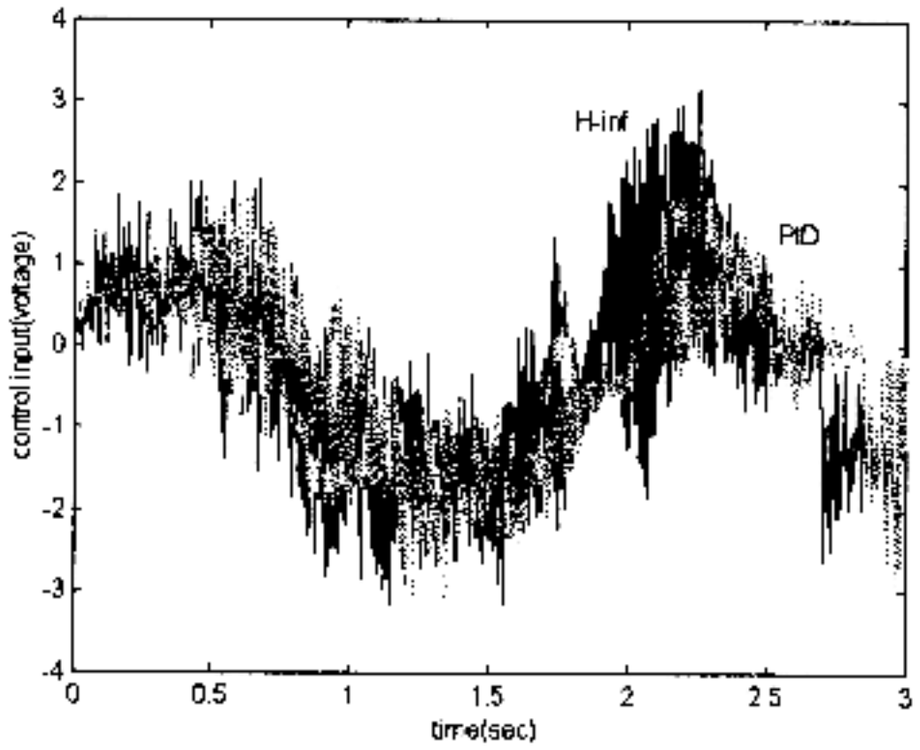

(b) Control input for the Y axis

Fig. 13 Comparison of the control inputs.

1997), their absolute values are about 1800 N/(m/sec) and exist inside of the allowable variation range for the designed MIMO controller. Contour error is defined as the distance from the reference trajectory to the output position. The maximum contour errors for both the axes are about 36 and 41 μm, respectively as shown in Fig. 10, in spite of high feed rate of the table.

The tracking performances of the MIMO controller and the PID controller in the cutting experiments are compared. The inner surface of the circle with the radius of 30 mm is cut by using the PID controller. The cutting tool will be less embedded in the workpiece when it cuts the inner surface of the larger circle as shown in Fig. 11. The less cutting force may be reflected to the PID controller than the MIMO controller which cut the circle with the radius of 28mm.

Figure 12 shows the tracking performance of the MIMO controller and PID controller for cutting circles. The contouring error in the Fig. 12 (c) is magnified to 300 times of its actual size. The MIMO controller demonstrates considerably better performance for both axes than the PID controller. The PID controller induces larger error at about 1.4 sec for the X-axis and 1.24 sec for Y-axis when the axes reverse their moving directions. Figure 13 shows control inputs to the power amplifiers of the linear motors. The control input of the PID controller for X axis is higher than that of the MIMO controller in most region. It demonstrates that the MIMO controller can control the X-axis better than the PID controller with less control input. The MIMO controller needs a little more control input for the Y axis.

6. Conclusions

In this work, a MIMO H_∞ controller for the linear motor machine tool feed drives has been designed to reduce tracking errors induced by cutting forces for end milling. The controller was designed using normalized coprime factorization method and by considering constant cutting force gain to give coupling effects between X and Y axes. Simulation results showed that the MIMO controller allows less tracking error than the PID controller, even though both controllers have similar size of the structured singular values for robust stability. The designed controller was directly implemented on a linear motor X-Y table via a DSP board. The table was mounted on a milling machine to have cutting experiments. Experiments were performed to verify the superior performance of the MIMO controller over the PID controller.

The MIMO controller demonstrated good performance in the cutting condition of the high feed rate and high spindle speed, while the PID controller brought about considerably large tracking error. The experimental results of the air and real cutting showed robustness of the MIMO controller for wide range of the cutting force and feed rate changes.

References

Alter, D. M. and Tsao, Tsu-Chin, 1994, "Stability of Turning Processes with Actively Controlled Linear Motor Feed Drives," *ASME Journal of Engineering for Industry*, Vol. 118, pp. 649~656.

Alter, D. M. and Tsao, Tsu-Chin., 1996, "Control of Linear Motors for Machine Tool Feed Drives," *ASME Journal of Dynamic Systems, Measurement and Control*, Vol. 118, pp. 649~656.

Balas, G. J. et al, 1991, *μ-Analysis and Synthesis Toolbox*, The Mathworks, Inc.

DeVor, R. E., Kline, W. A. and Zdeblick, W. J., 1980, "A Mechanistic Model for the Force System in End Milling with Application to Machining Airframe Structures," *Proceedings of the NAMRC8*, SMC, pp. 297~303.

Golub, A. D., 1992, "Unified Process Planning and Coordinated Motion Optimization for Multi-Axis Machines in High Speed Milling," Ph. D Thesis, Department of Mech., Aero. and Nucl. Eng., University of California, Los Angeles.

Zhou, K., 1997, *Robust and Optimal Control*, Prentice Hall, Inc.

Glover, K. and McFarlane, D. C., 1989, "Robust Stabilization of Normalized Coprime factor Plant Descriptions with Bounded Uncertainty," *IEEE Trans. Automat. Contr*, Vol. 34, No. 8, pp. 821~830.

McNab, R. J., 1997, "Digital Tracking Control for Machine Tool Feed Drives," Ph. D Thesis, Department of Mech., and Indus. Eng., University of Illinois at Urbana-Champaign.

Tlusty, J. and MacNeil, P., 1975, "Dynamics of Cutting Forces in End Milling," *Annals of the CIRP*, Vol. 24.